Dynamic impedance measurements of the Direct Methanol Fuel Cell cathode at various operating temperatures

L. Gawel [*], D. Parasinska

Department of Electrochemistry Corrosion and Materials Engineering, Faculty of Chemistry, Gdansk University of Technology, 11/12 Narutowicza Street, 80-233, Gdansk, Poland

A R T I C L E   I N F O

A B S T R A C T

This article presents results about the catalytic activity of the cathode in a Direct Methanol Fuel Cell (DMFC) across various operating temperatures. The Dynamic Electrochemical Impedance Spectroscopy (DEIS) technique coupled with a linear current scan was applied for this purpose. An equivalent model based on the thin-film flooded agglomerate model describing the cathode's behaviour was presented, and changes in its parameters were compared with the current load and different temperatures. Studies reveal shifts in cathodic kinetics with increasing load and temperature, alongside changes in resistance curves' slopes. The study identifies 351 K as the most optimal temperature, impacting parameters such as carbon layer resistance, diffusion parameter 1/Yo, and double electric layer capacitance significantly. Differences in slopes of resistance changes for different temperatures were also observed.

1. Introduction

The main sources of hydrogen carriers used in Proton Exchange Membrane (PEM) fuel cells so far are natural gas and fossil fuels. However, there is a possibility of producing liquid carriers from renewable biofuels as well [1,2]. Among them, the most important liquid hydrogen carriers that can be used for energy production in fuel cells include methanol, ethanol, formic acid, and ammonia. Their advantage, unlike pure hydrogen, is the ease of storage and transport. By using methanol as a direct power source in Direct Methanol Fuel Cells (DMFC) or formic acid in Direct Formic Acid Fuel Cells (DFAFC), new possibilities have opened up for the development of mobile power devices, providing competition for popular batteries characterized by for example, long charging times.

The most popular technique used for research on materials applied in fuel cells is cyclic voltammetry [3–6]. The obtained voltammograms allow the determination of reactions occurring at the electrode during the fuel cell's operation. However, in most studies, liquid electrolytes such as H_2SO_4 or $HClO_4$ are used for this purpose. Unfortunately, results obtained in this way do not always directly correspond to the behaviour under real operating conditions of fuel cells, where other factors come into play, such as the influence of the properties of the membrane in DMFC, DFAFC, and other cells. Other popular techniques for

measurement of the performances of the DMFC and DMFC cathodes are linear sweep voltammetry and open circuit voltage measurements [7–10]. The interesting behaviour of the DMFC in the magnetic field was presented by Celik et al. [11]. Also in the field of the flow field design presents a novel approach [12]. Zago et al. [13] in their paper focused on the methanol crossover process to cathode with a novel approach to the measurement of the OCV test and impedance with a reference electrode. They observed that reduction of total resistance with increasing methanol crossover. Another approach of the external reference electrode has been applied by Rabissi et al. [14] to identify variations of the electrode potential across the active area of the cell.

The Electrochemical Impedance Spectroscopy (EIS) technique is another method commonly used in research on fuel cells [15,16]. To determine changes in impedance under the influence of varying operating conditions, researchers such as Nakagawa et al. [17], Amphlett et al. [18], and Diard et al. [19] have applied this technique. One of the challenges encountered during the operation of direct methanol fuel cells is the occurrence of the crossover. This happens when methanol molecules diffuse through the membrane and are directly oxidized by oxygen from the cathode zone [20]. It is a significant issue that substantially reduces the fuel cell's voltage, maximum current density, fuel consumption, and consequently, the overall efficiency of the fuel cell [21,22].

---

* Corresponding author.
E-mail address: lukasz.gawel@pg.gda.pl (L. Gawel).

The aforementioned studies on fuel cells based on the EIS technique assume the system's stationarity throughout the entire measurement duration. To achieve this, prolonged conditioning of the tested system is required, leading to the omission of dynamic changes in the system related, for example, to variations in flow rate, temperature, or momentary changes in current load. By combining linear sweep voltammetry with the technique of Dynamic Electrochemical Impedance Spectroscopy (DEIS) [23–26], impedance spectra of the fuel cell were obtained under real operating conditions, depending on factors such as reagent flow rate, temperature, or current load changes. The comparison between the use of the DEIS and EIS techniques was straightforwardly presented by Darowicki [27].

In the case of fuel cells, the main element causing voltage losses is the cathode [23]. Moreover, the value of the anodic exchange current density, which corresponds to the rate of the methanol oxidation reaction is approximately 3 orders of magnitude higher than the oxygen reduction reaction at the cathode (ORR) [28,29]. Impedance studies on the behaviour of the ORR at the cathode are commonly used [30]. The most detailed description of the electrode behaviour with a diffusive layer is presented in the thin-film flooded agglomerate model proposed by Raistrick et al. [31,32]. In this model, the catalyst layer applied on the electrochemical surface of a neutral substrate is considered a group of agglomerates filled with electrolytes and covered on the outer side by a thin layer of pure electrolyte. The agglomerates are embedded in open hydrophobic channels, through which the oxidant reaches by first overcoming the thin layer of electrolyte on the surface and then diffusing into the interior of hydrophobic pores. As a result, a concentration gradient is formed along the pore. The EIS technique is rarely used to determine the validity of this model, but Ciureanu et al. [33] employed impedance techniques. They demonstrated that obtaining three semi-circles responsible for the charging of the double layer, the dynamics of the process, and oxygen diffusion through the thin film under real conditions is not possible, as in stationary studies [31]. There are few publications providing evidence for the existence of two loops at high overpotentials. The low-frequency loop seems to be the most interesting as it may provide information about the diffusion process, largely responsible for the total resistance of cathodic processes. However, the origin of this loop is controversial since it is assigned to slow oxygen diffusion through the substrate layer, water diffusion through the membrane, or water diffusion in the catalyst layer [34–36].

This work aims to assess the catalytic activity of the cathode in a DMFC in different operation temperatures due to the fact, that the cathodic process is the rate-determining process in the DMFC. The DEIS technique coupled with linear voltammetry was used for this purpose, allowing for the evaluation of the fuel cell cathode under real, non-stationary conditions. This technique allows for simultaneous recording of impedance value changes during load variation. By evaluating the cell's behaviour at different temperatures and varying loads, it is possible to determine changes in cathode parameters, and kinetics during load changes. A technical equivalent circuit, considering the influence of the diffusion layer on the ORR process in the operating cell was used. A change in the kinetics of cathodic processes was observed with increasing load, as well as the influence of temperature on the shift of these processes in the fuel cell. Changes in the slope of the resistance curves with increasing load have been observed, which has not been presented in the literature yet. This novel of the cathode measurements allows us to obtain the resistance changes during the time of the experiment. Differences in slopes depending on temperature were also recorded. Through the assessment of individual parameters, it is possible to determine the optimal load and temperature at which the DMFC cell exhibits the best properties, as well as evaluate the parameters determining the processes occurring during ORR at the cathode.

2. Experimental

A commercial DMFC cell with an active surface area of 1 cm^2 was used for the experiment. The membrane electrode assembly (MEA) consisted of a Nafion 117 membrane (thickness 183 μm), a cathode with 4 mg/cm^2 Pt on a carbon support, and an anode with 4 mg/cm^2 Pt/Ru also on a carbon support. The gas diffusion layer was a hydrophobized carbon with a 10 wt% polytetrafluoroethylene (PTFE) loading at the cathode and a 5 wt% PTFE loading at the anode.

The MEA was positioned between two graphite covers with 1×1 mm channel geometry in a serpentine pattern. The fuel was a 1 M methanol solution supplied to the cell using a peristaltic pump (Colepalmer Masterflex L/S) at a rate of 0.1 ml/min. The cathodic zone was fed with oxygen (>99, 5% purity) at a flow rate of 10 ml/min, controlled by a mass flow controller (Brooks MFC 5850 E). The higher flow was aimed at avoiding diffusion losses associated with a limited supply of the reactant to the cell, only considering losses related to the geometry of the cell itself.

To monitor the cathodic process, a pseudoreference Ag/AgCl electrode with a diameter of 0.25 μm was introduced into the cell (Fig. 1a). The electrode was placed at the anode/membrane interface, and additionally, the location of the reference electrode was separated from the bipolar plate by placing a Teflon gasket. Thanks to this, it was also possible to observe changes in the membrane resistance. The measurements were conducted using the technique of DEIS coupled with linear sweep voltammetry (LSV). In galvanostatic impedance studies, a multisine excitation ranging from 6.3 kHz to 900 mHz was employed, generated by the PXI-4461 card. The amplitude and phase shifts of the components were adjusted to ensure that the voltage amplitude of the variable signal did not exceed 10 mVpp (peak to peak) during the measurement. This signal was input into AUTOLAB 302 N, where it was summed with a constant current signal and then applied to the tested fuel cell. Using an additional PXI-4462 card, between the cathode and the pseudoreference electrode. Through the use of a short-time Fourier transform, spectra were obtained during dynamic changes in the parameters of the fuel cell. The rate of change in the current load was set at 50 μA/s. In the case of continuous variation of cell load, it would not be possible to obtain the presented results using the classical EIS technique. Measurements were conducted until the potential value of the investigated fuel cell reached 50 mV. The measurement was performed at three temperatures: 325 K, 338 K, and 351 K, using the LIM N1200 temperature controller after prior stabilization of the cell's operation at each temperature. The higher temperature values were not tested by the specifications provided by the MEA manufacturer. The declared maximum operating temperature was 353 K.

A simplified schematic diagram of the fuel cell construction, along with the positioning of the pseudoreference electrode, is presented in Fig. 1a. Fig. 1b presents an equivalent circuit with two active sites: a carbon support layer and active sites consisting of platinum as a catalyst.

In Fig. 1c–a simplified equivalent circuit is presented, which was used to analyse the obtained impedance spectra [23]. The analysis was carried out using the commercial tool ZSimpWin.

3. Results and discussion

The cathode current-voltage curve recorded with the pseudoreference electrode placed on the opposite side of the membrane (Fig. 1a) at different temperatures is presented in Fig. 2. An increase in cathode efficiency was observed with the rise in the operating temperature of the cell, which is thermodynamically justified. The maximum current density achieved under the polarization of the entire cell (between the covers) to a minimum voltage of 50 mV was approximately 140 mA/cm^2. In the case of an increase in temperature from 325 K to 338 K, no significant changes in potential were observed at the same load. However, an increase in temperature to the range of 351 K resulted in a substantial increase in the cathode potential.

The proposed two-dimensional model (Fig. 1b) assumes that the course of the ORR may be concurrently influenced not only by the catalytic layer (active sites) but also by the support carbon along with the
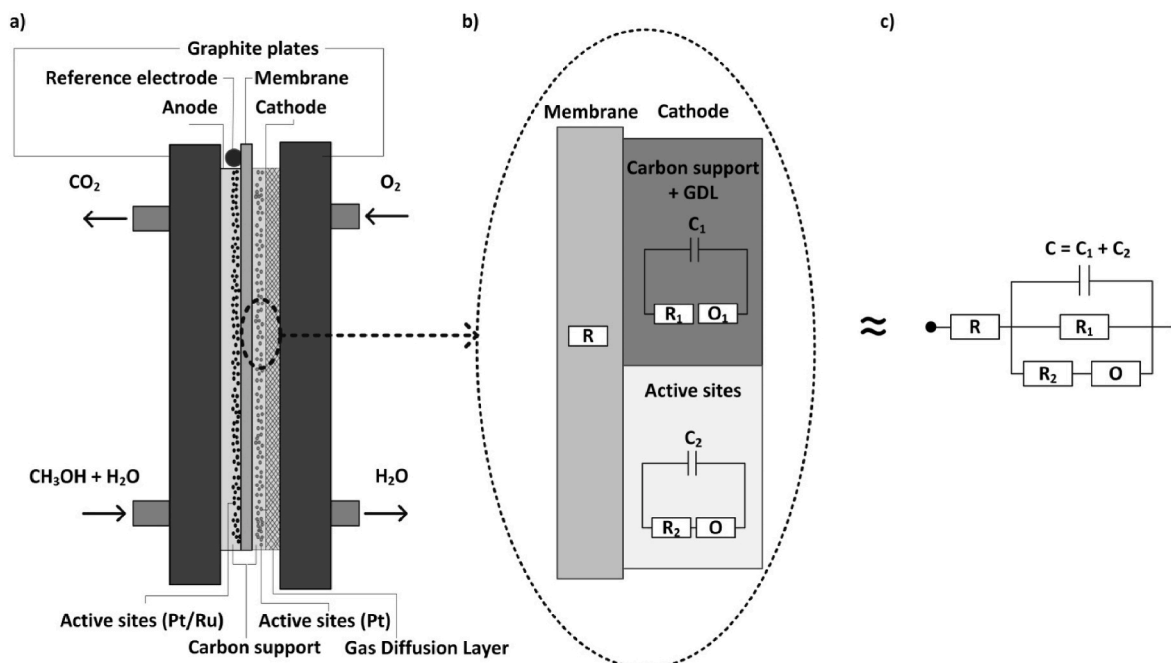
Fig. 1. a) Simplified schematic diagram of a DMFC b) Equivalent circuit of the cathode with two active regions participating simultaneously in the reduction process and a membrane c) Optimized equivalent circuit used for the analysis of obtained impedance spectra.
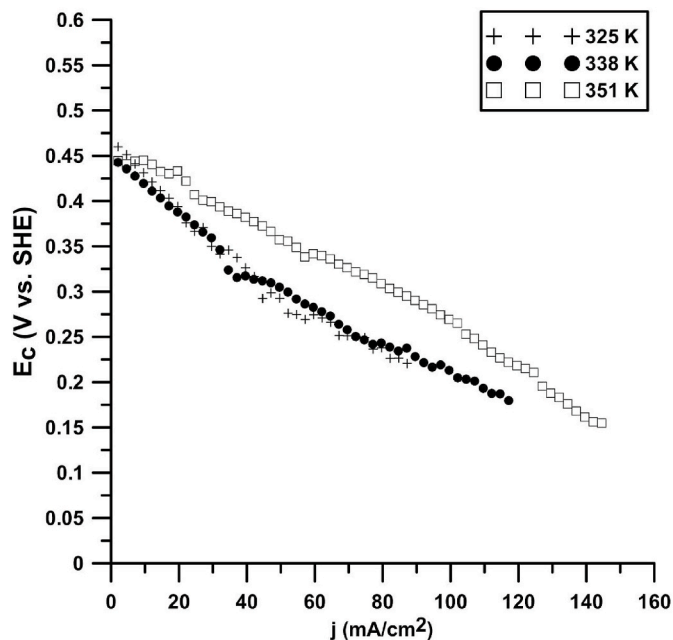

Fig. 2. Characteristics of the cathode potential for temperatures: 325 K, 338 K, and 351 K relative to the Standard Hydrogen Electrode (SHE).

diffusion layer, both having an approximate composition. The total impedance of the cathode will thus consist of resistance R - responsible for the membrane resistance and electrolyte diffusion through the membrane in the crossover process, capacitances C_1, C_2 - describing the double-layer capacitance on the carbon support and the catalyst, charge transfer resistance on the carbon R_1 [37], charge transfer resistance on the catalyst layer R_2, and parameters O_1 and O responsible for the diffusion process of the reactant through the porous layer of finite length. According to the assumptions, the resistance R_1 responsible for the reduction process on the carbon support should be characterized by relatively high values. In the case of the catalyst, the charge transfer

process should exhibit lower resistance (R_2). Accordingly, for the catalyst layer, it is also necessary to consider the influence of diffusion through the porous layer of finite length (O) on the rate of ongoing processes. However, in the examined frequency range (6.3 kHz - 900 mHz), during dynamic changes in operating conditions, it is not possible to accurately determine the parameter O1 responsible for the diffusion process in the carbon layer, as the electroreduction process may occur over a relatively large surface compared to platinum agglomerates. At the same time, it is assumed that the capacitance of the double electric layer is uniform throughout the cathode space and, consequently, is the sum of the partial capacitances C_1 and C_2.

Measurements were conducted at various temperatures using the DEIS technique with simultaneous variation of the load. In Figs. 3–5, the changes in cathode impedance with increasing load at three temperatures: 325 K, 338 K, and 351 K are presented. The impedance of the cathode decreases with increasing load for all examined temperatures. The spectra exhibit the shape of flattened semicircles with a linear range at high frequencies (Figs. 3b, 4b and 5b).

At low current densities, a second time constant becomes apparent in the low-frequency range. Additionally, a gradual decrease in impedance with increasing temperature can be observed, indicating the influence of temperature on the efficiency of the cathodic process.

The impedance spectra analysis using the proposed equivalent circuit is characterized by a fitting level chi^2 in the range of 10^{-4} to 10^{-5}, indicating a good correlation between experimental results and reference spectra.

The capacitance of the double layer C (Fig. 6), representing the sum of the capacitance on the carbon support and the active sites, exhibits a similar characteristic for all temperatures. Upon reaching a certain current value at the beginning of the current load changes, values decreasing, and further load increase do not significantly affect achieving the minimum. The minimum value for temperatures 325 K and 338 K was achieved at around 70 and 80 mA/cm^2. In the case of a temperature of 351 K, the largest decrease in capacitance values was observed (approximately 0.4 mF), as well as a shift in the minimum value, which was achieved at around 100 mA/cm^2. The increase in capacitance values at higher loads may be caused by a change in the reaction determining the oxygen reduction process, after which there is
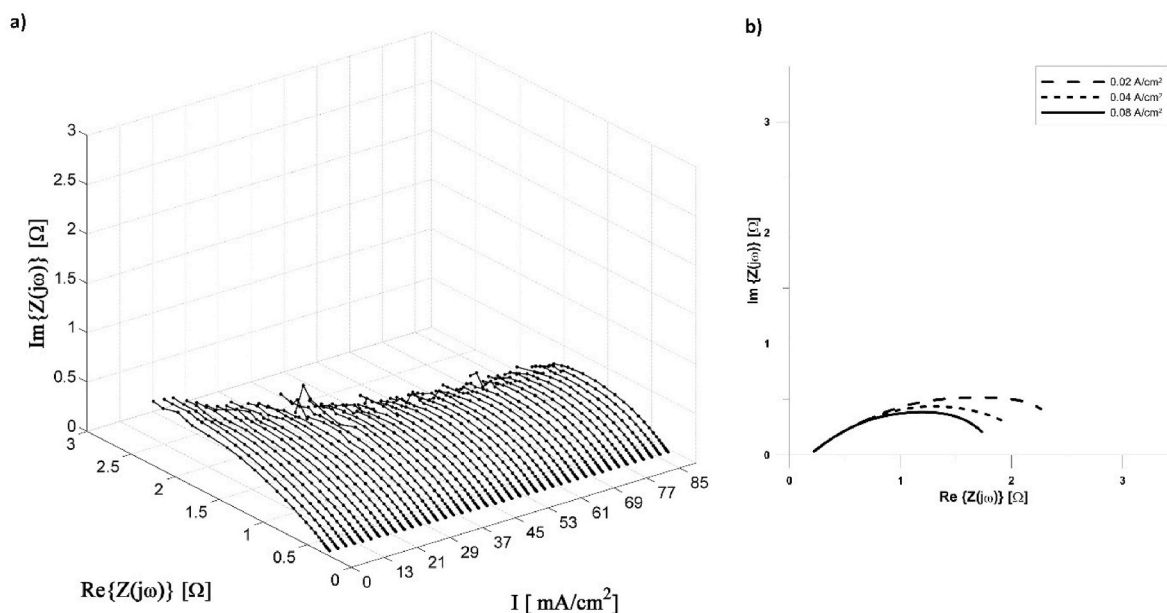
Fig. 3. a) Impedance spectrum of the cathode with changing load. b) Individual spectrograms obtained by the DEIS technique for various current density values at 325 K.
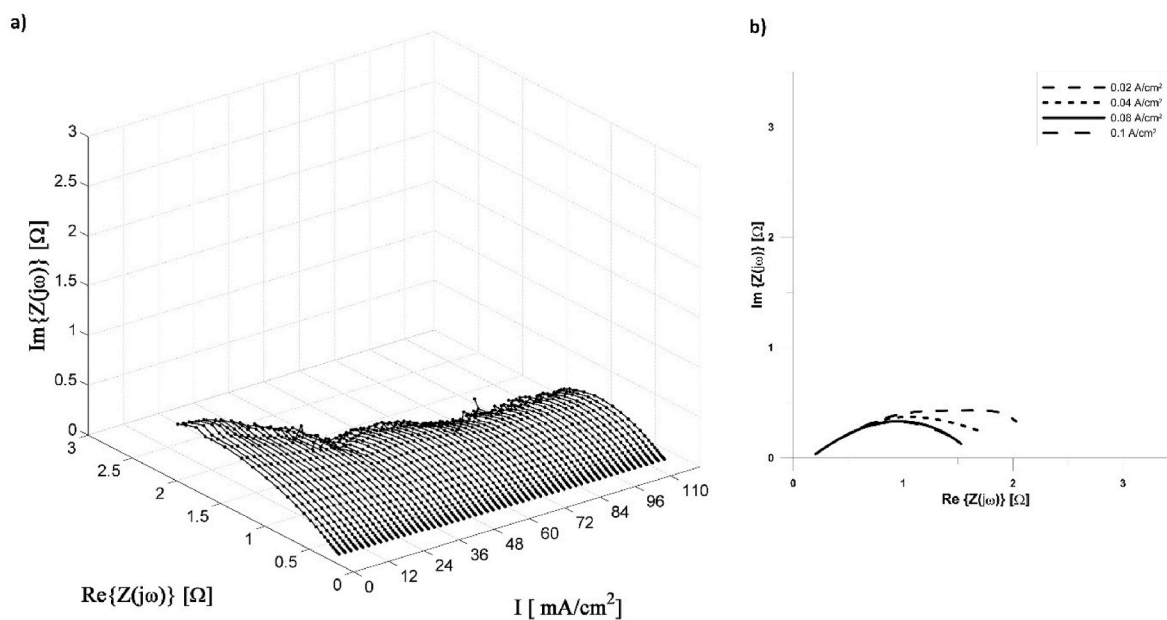

Fig. 4. a) Impedance spectrum of the cathode with changing load. b) Individual spectrograms obtained by the DEIS technique for various current density values at 338 K.

a subsequent increase in the electrode's capacitance and an increase in the amount of adsorbed particles on the electrode surface. The increasing amount of water and accumulation related to the cell geometry or the crossover process can also be the cause of this change.

The linear decrease in the values of membrane resistance R (Fig. 7) was observed for temperatures 325 K and 338 K. The linear relationship is directly associated with the ohmic resistances of the cell. The maximum change in resistance with increasing load was observed at a temperature of 351 K and is approximately 80 mΩ. The decrease in resistance with temperature is due to the increased mobility of charge carriers through the membrane. The linear trend suggests that even at a temperature of 351 K, membrane drying does not occur, which can contribute to the loss of ionic conductivity.

The dependency of polarization resistance changes of carbon support R_c (Fig. 8) and active sites R_{Pt} (Fig. 9), can be divided into two linear regions differing in slope. In the case of the first region, the change with increasing current density is more abrupt and characterized by a steeper slope compared to the second region. The larger drop is likely caused by the reduction of surface oxides adsorbed on the cathode surface, a process faster than the reduction of non-adsorbed oxygen. A direct consequence of the change in the reactant is a decrease in power observed for higher load values. With an increase in temperature, a significant decrease in the slope value of both resistances was observed.

Comparing the values of resistances R_C and R_{Pt} (Figs. 8 and 9), it can be observed that the charge transfer resistance at the active sites is almost two orders of magnitude smaller than the resistance of the carbon
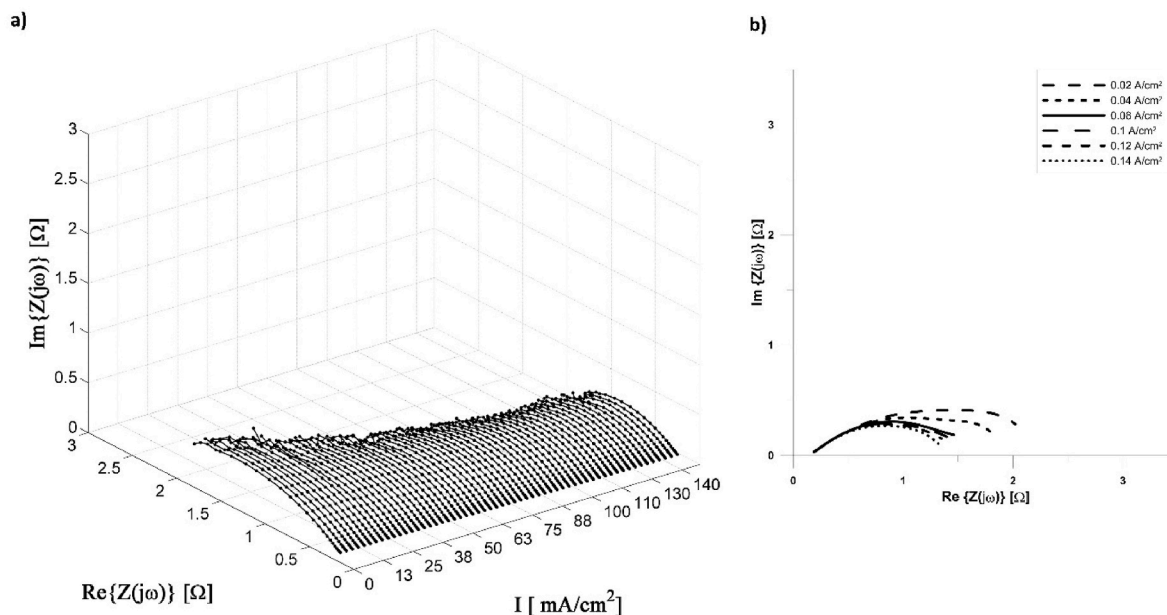
Fig. 5. a) Impedance spectrum of the cathode with changing load. b) Individual spectrograms obtained by the DEIS technique for various current density values at 351 K.
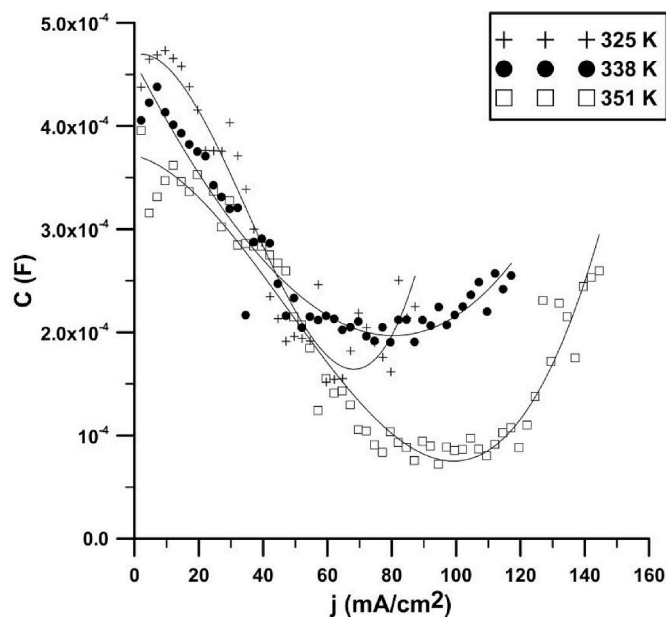

Fig. 6. Change in the sum of the double-layer capacitance of the carbon support and active centres depending on the load.

Fig. 7. Change in membrane resistance with the increase of the current load.

support. This is associated with the speed of the ORR, where the rate on platinum nanoparticles is significantly higher than on carbon. In the case of the parallel connection of these two parameters, it follows that the charge transfer process on the catalytic layer is the determining factor for the electroreduction of oxygen at the cathode.

In Table 1, the results of changes in slope values and intercept values are presented as a function of temperature for individual resistance values. For charge transfer resistance values R_C and R_{Pt}, the values of two linear dependencies were presented, namely a_1 and b_1 corresponding to the low current density range, and a_2 and b_2 corresponding to the higher current density range. For values of charge transfer resistance of carbon support in the low current range, a decrease in the slope exceeding 57% was observed with increasing temperature. In the case of
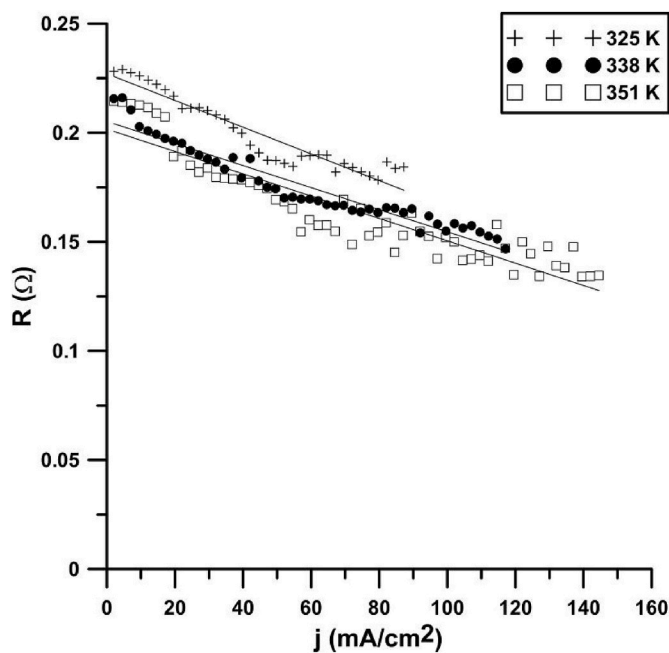
the high-current part, this decrease was about 43%. Moreover, significant shifts of the curves towards lower values were also observed. The value of charge transfer resistance on platinum in the low-current range does not exhibit such a significant change, and it is approximately 36%, while in the high-current range, a similar dependence to the change in the slope of the carbon support was observed (about 44%). Compared to the carbon carrier, no significant shift in curve resistance values was observed with an increase in temperature as well. Results indicate a much greater influence of temperature on ORR on carbon support and for both materials in the low-current range, where the dominant limit is activation losses, compared to higher current loads. In the case of changing the slope of the membrane resistance (R), no significant impact on the change in the slope was observed. Only a shift in the resistance
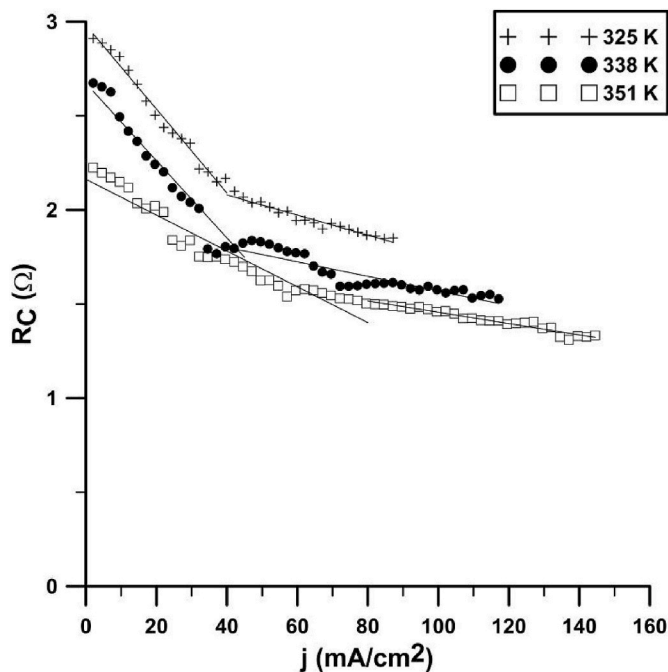
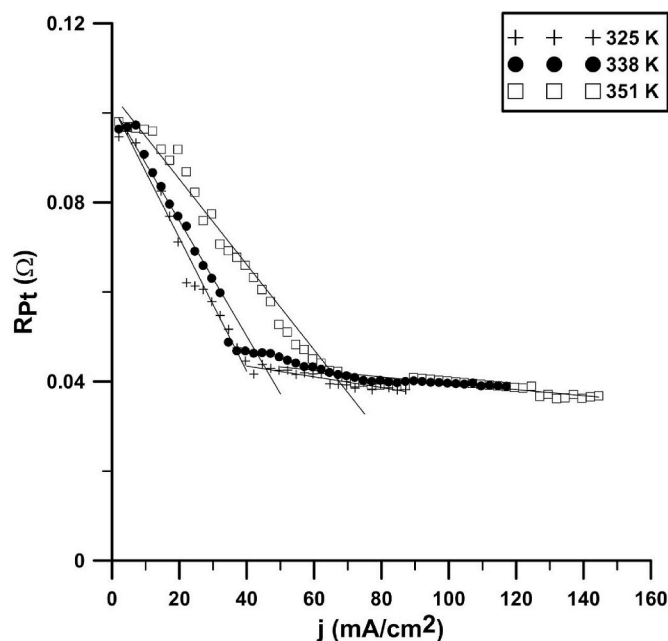**Fig. 8.** Dependency of carbon support polarization resistance changes with the increase of the load.

Fig. 9. Dependency of active sites polarization resistance changes with the increase of the load.

Table 1
Change in the slope and intercept values for different resistances.

Element	T [K]	a_1	b_1	a_2	b_2
Rc	325	−22.293	2.959	−5.337	2.293
	338	−20.543	2.747	−3.877	1.957
	351	−9.526	2.163	−3.006	1.757
R_{Pt}	325	−1.485	0.102	−0.120	0.048
	338	−1.286	0.102	−0.074	0.047
	351	−0.953	0.104	−0.068	0.046
		a		**b**	
R	325	−0.612		0.227	
	338	−0.506		0.205	
	351	−0.512		0.202	

$$Z_o = \frac{1}{Y_O\sqrt{j\omega}}\tanh\left(B\sqrt{j\omega}\right) \tag{1}$$

where $B = \delta/D^{1/2}$, D-the diffusion coefficient, δ-the thickness of the electrolyte, Z_o – impedance of diffusion process through the porous layer with a finite length for platinum catalyst, Y_o-admittance of diffusion process, ω-angular frequency.

The relationship between the changes in $1/Y_o$ with the load is shown in Fig. 10. With an increase in temperature, the parameter values increase. Each graph can be divided into two linear regions. The first one is characterized by a constant value until a certain critical current is reached, after which there is a decrease in the value of the inverse admittance $1/Y_o$. With an increase in temperature, the current density at which the value decreases also increases. The initial constant value region may be due to the initial reduction of surface oxides, causing the amount of oxygen delivered to the catalyst surface to have little impact on the electroreduction process. However, with an increase in load and a decrease in the amount of adsorbed oxides, the demand for molecular oxygen increases, leading to a decrease in the value of the inverse admittance.

The last of the discussed parameters is the parameter B (Fig. 11), which has a direct correlation with the diffusion coefficient and the thickness of the diffusion layer. Changes in temperature and increasing load do not affect the parameter B. Therefore, it can be considered
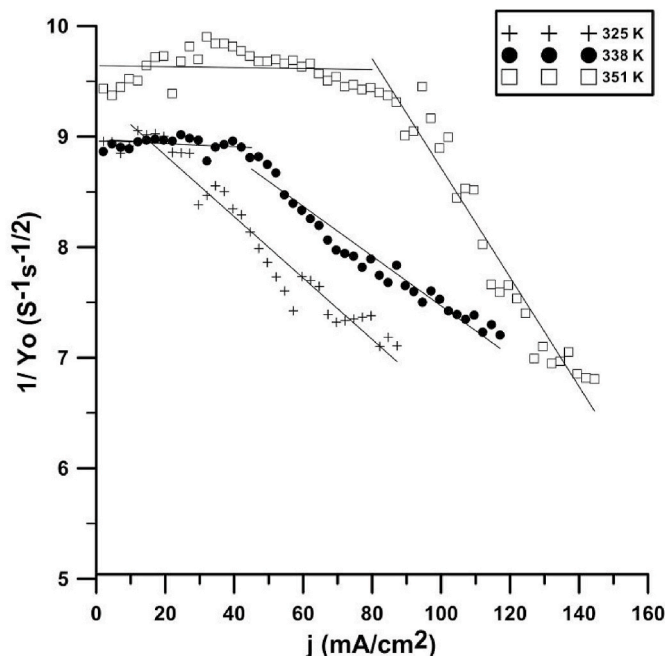
values towards lower values was noticed with an increase in temperature.

Due to the very low values of resistance R_{Pt}, it was reasonable to assume that in the model describing the active sites, an additional parameter related to diffusion through the porous layer of finite length in the electrochemical process of oxygen reduction on the Pt electrode should be considered. In the case where oxygen is the electrolyte, the diffusion area is limited by the thickness of the diffusion layer and the length of the pores in the support layer. In such conditions, the parameter O should be described as:

Fig. 10. The dependency of the change of $1/Y_o$ values on the change in current load.
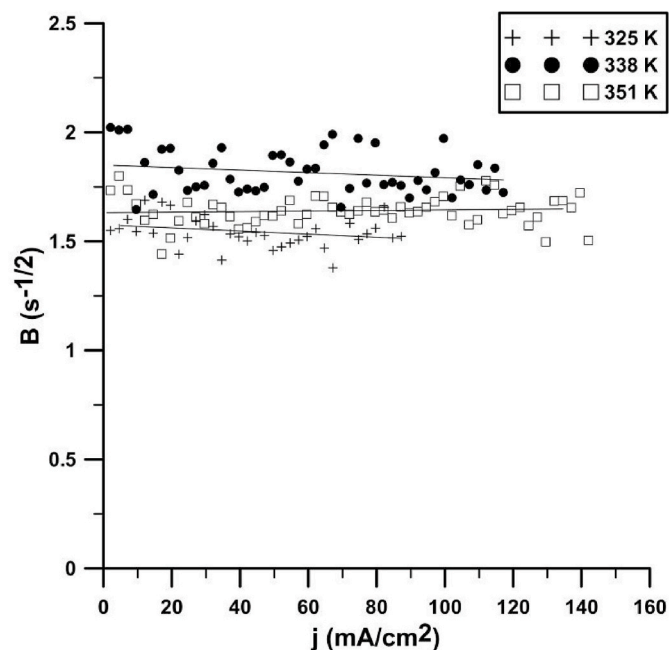
Fig. 11. The dependency of the change of B values on the change in current load.

constant for current load changes. Since the diffusion layer is compressed between the covers, its thickness and the influence of temperature on its change cannot be unequivocally determined. Assuming that the change in thickness of the layer is negligibly small for all temperatures, the diffusion coefficient of reactants through the porous layer remains constant with increasing load.

4. Conclusions

The research was conducted at three different operating temperatures of the fuel cell, with varying loads. The application of DEIS allowed for obtaining the response of impedance changes in the investigated system along with the dynamic variation of operating conditions in the cell. The results obtained from the study on the cathode properties in a fuel cell operating under real working conditions demonstrate that DEIS coupled with constant current techniques is a good tool for investigating the influence of variable conditions on the properties of cell components. This is not possible with constant current methods or the alternative classical EIS technique, where system stability is required during the measurement. The obtained results also indicate the correct placement of the reference electrode in the cell, allowing it to be used in the future for research on other operational parameters.

The obtained temperature dependencies suggest that the temperature of 351 K is the most optimal among those presented in the above work. Simultaneously, the temperature has the greatest influence on the change in the resistance of the carbon layer, the diffusion parameter $1/Y_o$, and the capacitance of the double electric layer.

According to the obtained results, it can be concluded that the process determining the cathode performance is the charge transfer process on the catalyst, where the parallel resistance has also the lowest values. In addition, the presence of two linear regions during the change in cell load was observed in most parameters, which may be caused by a change in the reduction process of surface-adsorbed oxygen species to the reduction of molecular oxygen supplied to the cell. The ORR is a complex phenomenon, as evidenced by numerous literary reports and this can have a direct impact on the overall power decrease of the fuel cell. This analysis requires further complex research, encompassing the study of both DMFC cathode and anode behaviour, as well as investigating changes in operating conditions, such as methanol concentration

or reagent flow rates. It may directly contribute to the changes occurring within the cell and demonstrate intriguing relationships among impedance parameter changes, thereby advancing our understanding of the behaviour of these devices.

CRediT authorship contribution statement

L. Gawel: Conceptualization, Formal analysis, Methodology, Resources, Software, Supervision, Validation, Writing – original draft, Writing – review & editing. **D. Parasinska:** Data curation, Investigation, Methodology, Visualization, Writing – original draft, Writing – review & editing.

Declaration of competing interest

The authors declare that they have no known competing financial interests or personal relationships that could have appeared to influence the work reported in this paper.

References

[1] Vlysidis A, Binns M, Webb C, Theodoropoulos C. Glycerol utilisation for the production of chemicals: conversion to succinic acid, a combined experimental and computational study. Biochem Eng J 2011;58–59:1–11. https://doi.org/10.1016/j.bej.2011.07.004.

[2] Twidell J, Weir T. Renewable energy Resources. 0 ed. Routledge; 2015. https://doi.org/10.4324/9781315766416.

[3] Marković NM, Gasteiger HA, Ross PN, Jiang X, Villegas I, Weaver MJ. Electro-oxidation mechanisms of methanol and formic acid on Pt-Ru alloy surfaces. Electrochim Acta 1995;40:91–8. https://doi.org/10.1016/0013-4686(94)00241-R.

[4] Wang B. Recent development of non-platinum catalysts for oxygen reduction reaction. J Power Sources 2005;152:1–15. https://doi.org/10.1016/j.jpowsour.2005.05.098.

[5] Wang X, Li W, Chen Z, Waje M, Yan Y. Durability investigation of carbon nanotube as catalyst support for proton exchange membrane fuel cell. J Power Sources 2006;158:154–9. https://doi.org/10.1016/j.jpowsour.2005.09.039.

[6] Raso MA, Carrillo I, Navarro E, Garcia MA, Mora E, Leo TJ. Fuel cell electrodes prepared by e-beam evaporation of Pt compared with commercial cathodes: electrochemical and DMFC behaviour. Int J Hydrogen Energy 2015;40:11315–21. https://doi.org/10.1016/j.ijhydene.2015.03.125.

[7] Zhang H, Liu Z, Gao S, Wang C. A new cathode structure for air-breathing DMFCs operated with pure methanol. Int J Hydrogen Energy 2014;39:13751–6. https://doi.org/10.1016/j.ijhydene.2014.02.145.

[8] Monteverde Videla AHA, Sebastián D, Vasile NS, Osmieri L, Aricò AS, Baglio V, et al. Performance analysis of Fe–N–C catalyst for DMFC cathodes: effect of water saturation in the cathodic catalyst layer. Int J Hydrogen Energy 2016;41:22605–18. https://doi.org/10.1016/j.ijhydene.2016.06.060.

[9] Chikumba FT, Tamer M, Akyalçın L, Kaytakoğlu S. The development of sulfonated polyether ether ketone (sPEEK) and titanium silicon oxide (TiSiO4) composite membranes for DMFC applications. Int J Hydrogen Energy 2023;48:14038–52. https://doi.org/10.1016/j.ijhydene.2022.12.293.

[10] Li X, Miao Z, Marten L, Blankenau I. Experimental measurements of fuel and water crossover in an active DMFC. Int J Hydrogen Energy 2021;46:4437–46. https://doi.org/10.1016/j.ijhydene.2020.11.027.

[11] Çelik S, Yagız M, Atalmis G. Experimental improvement of the performance of the open cathode-direct methanol fuel cell stack by magnetic field effect. Int J Hydrogen Energy 2024;50:32–40. https://doi.org/10.1016/j.ijhydene.2023.07.340.

[12] Okech G, Emam M, Mori S, Ahmed M. Enhancing the performance of direct methanol fuel cells using new cathode flow field designs: an experimental investigation. Int J Hydrogen Energy 2024;57:161–75. https://doi.org/10.1016/j.ijhydene.2024.01.015.

[13] Zago M, Bisello A, Baricci A, Rabissi C, Brightman E, Hinds G, et al. On the actual cathode mixed potential in direct methanol fuel cells. J Power Sources 2016;325:714–22. https://doi.org/10.1016/j.jpowsour.2016.06.093.

[14] Rabissi C, Brightman E, Hinds G, Casalegno A. In operando measurement of localised cathode potential to mitigate DMFC temporary degradation. Int J Hydrogen Energy 2018;43:9797–802. https://doi.org/10.1016/j.ijhydene.2018.04.043.

[15] Zhao X, Fan X, Wang S, Yang S, Yi B, Xin Q, et al. Determination of ionic resistance and optimal composition in the anodic catalyst layers of DMFC using AC impedance. Int J Hydrogen Energy 2005;30:1003–10. https://doi.org/10.1016/j.ijhydene.2005.01.006.

[16] Sun W, Zhang W, Su H, Leung P, Xing L, Xu L, et al. Improving cell performance and alleviating performance degradation by constructing a novel structure of membrane electrode assembly (MEA) of DMFCs. Int J Hydrogen Energy 2019;44:32231–9. https://doi.org/10.1016/j.ijhydene.2019.10.113.

[17] Nakagawa N, Xiu Y. Performance of a direct methanol fuel cell operated at atmospheric pressure. J Power Sources 2003;118:248–55. https://doi.org/10.1016/S0378-7753(03)00090-9.

[18] Amphlett JC, Peppley BA, Halliop E, Sadiq A. The effect of anode flow characteristics and temperature on the performance of a direct methanol fuel cell. J Power Sources 2001;96:204–13. https://doi.org/10.1016/S0378-7753(01)00490-6.

[19] Diard J-P, Glandut N, Landaud P, Le Gorrec B, Montella C. A method for determining anode and cathode impedances of a direct methanol fuel cell running on a load. Electrochim Acta 2003;48:555–62. https://doi.org/10.1016/S0013-4686(02)00722-3.

[20] Broussely M, Archdale G. Li-ion batteries and portable power source prospects for the next 5–10 years. J Power Sources 2004;136:386–94. https://doi.org/10.1016/j.jpowsour.2004.03.031.

[21] Han J, Liu H. Real time measurements of methanol crossover in a DMFC. J Power Sources 2007;164:166–73. https://doi.org/10.1016/j.jpowsour.2006.09.105.

[22] Du CY, Zhao TS, Xu C. Simultaneous oxygen-reduction and methanol-oxidation reactions at the cathode of a DMFC: a model-based electrochemical impedance spectroscopy study. J Power Sources 2007;167:265–71. https://doi.org/10.1016/j.jpowsour.2007.02.048.

[23] Darowicki K, Gawel L. Impedance measurement and selection of electrochemical equivalent circuit of a working PEM fuel cell cathode. Electrocatalysis 2017;8:235–44. https://doi.org/10.1007/s12678-017-0363-0.

[24] Darowicki K, Janicka E, Mielniczek M, Zielinski A, Gawel L, Mitzel J, et al. Implementation of DEIS for reliable fault monitoring and detection in PEMFC single cells and stacks. Electrochim Acta 2018. https://doi.org/10.1016/j.electacta.2018.09.105.

[25] Darowicki K, Janicka E, Mielniczek M, Zielinski A, Gawel L, Mitzel J, et al. The influence of dynamic load changes on temporary impedance in hydrogen fuel cells, selection and validation of the electrical equivalent circuit. Appl Energy 2019;251:113396. https://doi.org/10.1016/j.apenergy.2019.113396.

[26] Darowicki K, Gawel L, Mielniczek M, Zielinski A, Janicka E, Hunger J, et al. The impedance of hydrogen oxidation reaction in a proton exchange membrane fuel cell in the presence of carbon monoxide in hydrogen stream. Appl Energy 2020;279:115868. https://doi.org/10.1016/j.apenergy.2020.115868.

[27] Darowicki K, Ślepski P, Szociński M. Novel application of dynamic electrochemical impedance monitoring to a cataphoretic coating process. Prog Org Coating 2020;149:105906. https://doi.org/10.1016/j.porgcoat.2020.105906.

[28] Wang ZH, Wang CY. Mathematical modeling of liquid-feed direct methanol fuel cells. J Electrochem Soc 2003;150:A508. https://doi.org/10.1149/1.1559061.

[29] Sharifi S, Rahimi R, Mohebbi-Kalhori D, Colpan CO. Numerical investigation of methanol crossover through the membrane in a direct methanol fuel cell. Iran J Hydrogen Fuel Cell 2018;5. https://doi.org/10.22104/ijhfc.2018.2867.1170.

[30] Zhao X, Li W, Fu Y, Manthiram A. Influence of ionomer content on the proton conduction and oxygen transport in the carbon-supported catalyst layers in DMFC. Int J Hydrogen Energy 2012;37:9845–52. https://doi.org/10.1016/j.ijhydene.2012.03.107.

[31] Raistrick ID. Impedance studies of porous electrodes. Electrochim Acta 1990;35:1579–86. https://doi.org/10.1016/0013-4686(90)80013-E.

[32] Springer TE, Raistrick ID. Electrical impedance of a pore wall for the flooded-agglomerate model of porous gas-diffusion electrodes. J Electrochem Soc 1989;136:1594–603. https://doi.org/10.1149/1.2096975.

[33] Ciureanu M, Roberge R. Electrochemical impedance study of PEM fuel cells. Experimental diagnostics and modeling of air cathodes. J Phys Chem B 2001;105:3531–9. https://doi.org/10.1021/jp003273p.

[34] Springer TE, Zawodzinski TA, Wilson MS, Gottesfeld S. Characterization of polymer electrolyte fuel cells using AC impedance spectroscopy. J Electrochem Soc 1996;143:587–99. https://doi.org/10.1149/1.1836485.

[35] Paganin VA, Oliveira CLF, Ticianelli EA, Springer TE, Gonzalez ER. Modelisticinterpretation of the impedance response of a polymer electrolyte fuel cell. Electrochim Acta 1998;43:3761–6. https://doi.org/10.1016/S0013-4686(98)00135-2.

[36] Wagner N, Schnurnberger W, Müller B, Lang M. Electrochemical impedance spectra of solid-oxide fuel cells and polymer membrane fuel cells. Electrochim Acta 1998;43:3785–93. https://doi.org/10.1016/S0013-4686(98)00138-8.

[37] Qu D. Investigation of oxygen reduction on activated carbon electrodes in alkaline solution. Carbon 2007;45:1296–301. https://doi.org/10.1016/j.carbon.2007.01.013.